

# SPIN-DEPENDENT TRANSPORT IN PHASE-SEPARATED MANGANITES

K. I. Kugel, A. L. Rakhmanov, A. O. Sboychakov

*Institute for Theoretical and Applied Electrodynamics, Russian Academy of Sciences  
Izhorskaya str. 13/19, Moscow 125412, Russia*

kugel@orc.ru

M. Yu. Kagan, I. V. Brodsky, A. V. Klaptsov

*Kapitza Institute for Physical Problems, Russian Academy of Sciences  
Kosygina str. 2, Moscow, 119334 Russia*

**Abstract** Starting from the assumption that ferromagnetically correlated regions exist in manganites even in the absence of long-range magnetic order, we construct a model of charge transfer due to the spin-dependent tunnelling of charge carriers between such regions. This model allows us to analyze the temperature and magnetic field dependence of resistivity, magnetoresistance, and magnetic susceptibility of phase-separated manganites in the temperature range corresponding to non-metallic behavior. The comparison of theoretical and experimental results reveals the main characteristics of the phase-separated state.

**Keywords:** manganites, phase separation, spin-dependent tunnelling

## 1. Introduction

Unusual properties and the richness of the phase diagram of manganites gave rise to a huge number of papers dealing with different aspects of the physics of these compounds. A special current interest to manganites is related to the possible existence of various inhomogeneous charge and spin states such as lattice and magnetic polarons, droplet and stripe structures, etc. (Dagotto et al., 2001; Nagaev, 2001; Kagan and Kugel, 2001). Analogous phenomena are well known for many strongly correlated systems where the electron-electron interaction energy is higher than the kinetic energy. One of the most spectacular manifestations of such a behavior, i.e. the formation of ferromagnetic (FM) droplets

(ferrons) was predicted in Ref. (Nagaev, 1967) for low-doped antiferromagnetic (AFM) semiconductors. Another example is a formation of a string (linear trace of frustrated spins) upon the motion of a hole in an AFM isolator (Bulaevskii et al., 1968). Both these examples refer to the so-called electron phase separation, when a single charge carrier changes locally its electronic environment. In addition to this nanoscale phase separation, manganites can also exhibit a large-scale phase separation corresponding to the coexistence of different phases characteristic of first-order phase transitions (e.g., the transition between AFM and FM states). An example of this large-scale phase separation is given by the formation of relatively large FM droplets inside the AFM matrix. These droplets with linear sizes of about 100-1000 Å were observed in several experiments, in particular, by neutron diffraction methods in Ref. (Balagurov et al., 2001). Note also that the attraction between one-electron ferromagnetic droplets (mediated by either elastic or magneto-dipole interaction) can result in merging of the ferrons and formation of intermediate to large-scale inhomogeneities (Lorenzana et al., 2001). There exist clear experimental indications suggesting that the phase separation is inherent for both magnetically ordered phases and the paramagnetic state (Dagotto et al., 2001; Nagaev, 2001; Kagan and Kugel, 2001; Solin et al., 2003). Therefore, the formation of inhomogeneous states proved to be a typical phenomenon for manganites in different parts of their phase diagram. Moreover, the phase separation should strongly affect the magnetic and transport properties of manganites.

Phase separation arguments are most often used for the domain of the existence of antiferromagnetism and especially in the vicinity of a transition between AFM and FM states. However, as we mentioned earlier, a manganite can be inhomogeneous even in the paramagnetic state at temperatures exceeding the corresponding phase transition temperature. An analysis of experimental data reveals a substantial similarity in the high-temperature behavior of resistivity, magnetoresistance, and magnetic susceptibility for various manganites with different low-temperature states (Babushkina et al., 2003; Fisher et al., 2003; Wagner et al., 2002; Zhao et al., 2001). In addition, the magnetoresistance turns out to be rather large far from the FM-AFM transition and even in the paramagnetic region. Furthermore, the magnetic susceptibility of manganites is substantially higher than that for typical antiferromagnets. These experimental data clearly suggest the existence of significant FM correlations in the high-temperature range.

Here, we start from the assumption that the ferromagnetically correlated regions exist in manganites above the temperatures characterizing the onset of the long-range magnetic (FM or AFM) ordering. This

assumption allows us to describe the characteristic features of resistivity, magnetoresistance, and magnetic susceptibility of manganites in the non-metallic state within the framework of one model. Below, we base our discussion on the model of conductivity of phase-separated manganites developed in Ref. (Babushkina et al., 2003; Rakhmanov et al., 2001; Sboychakov et al., 2002; Sboychakov et al., 2003) and use experimental data for manganites of different compositions reported in Ref. (Babushkina et al., 2003; Fisher et al., 2003; Wagner et al., 2002; Zhao et al., 2001). Note that in this paper we do not limit ourselves by consideration of only one-electron magnetic droplets (ferrons) but rather generalize previously obtained results to the case of arbitrary number of electrons in ferromagnetically correlated domains.

In Section 2, the temperature dependence of resistivity is analyzed for the inhomogeneous state with the density of FM-correlated regions being far from the percolation threshold. In Sections 3 and 4, within the same assumptions, we discuss the magnetoresistance of manganites and their magnetic susceptibility, respectively. As a result, it is shown that the model of inhomogeneous state provides a good description for the high-temperature behavior of manganites. The comparison of theoretical results and experimental data allows us to reveal the general characteristics of ferromagnetically correlated regions.

## 2. Resistivity

In the analysis of the temperature dependence of resistivity, we will have in mind the physical picture discussed in the paper (Rakhmanov et al., 2001). That is, we consider a non-ferromagnetic insulating matrix with small ferromagnetic droplets embedded in it. Charge transfer occurs via tunnelling of charge carriers from one droplet to another. A tunnelling probability depends, strictly speaking, upon applied magnetic field. We assume that the droplets do not overlap and the whole system is far from the percolation threshold. Each droplet can contain  $k$  charge carriers. When a new charge carrier tunnel to a droplet, it encounters with the Coulomb repulsion from the carriers already residing at this droplet. The repulsion energy  $A$  is assumed to be relatively large ( $A > k_B T$ ). In this case, the main contribution to the conductivity is related to the processes involving the droplets containing  $k$ ,  $k + 1$ , or  $k - 1$  carriers. The corresponding expression for the resistivity  $\rho(T)$  has the form

$$\rho = \frac{k_B T \exp(A/2k_B T)}{128\pi e^2 \omega_0 l^5 k n^2}, \quad (1)$$

where  $e$  is the charge of the electron,  $\omega_0$  determines the characteristic energy of electrons in a droplet,  $l$  is the characteristic tunnelling length, and

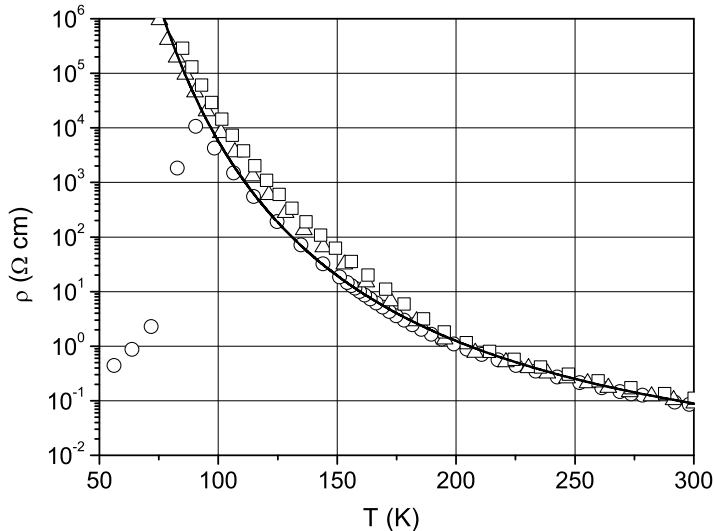


Figure 1. Temperature dependence of the resistivity for  $(\text{La}_{1-y}\text{Pr}_y)_{0.7}\text{Ca}_{0.3}\text{MnO}_3$  samples (Babushkina et al., 2003). Squares, triangles, and circles correspond to  $y = 1$  (with  $^{16}\text{O} \rightarrow ^{18}\text{O}$  isotope substitution),  $y = 0.75$  (with  $^{16}\text{O} \rightarrow ^{18}\text{O}$  isotope substitution), and  $y = 0.75$  (with  $^{16}\text{O}$ ), respectively. Solid line is the fit based on Eq. (1).

$n$  is the concentration of ferromagnetic droplets. Expression (1) could be easily derived by the method described in Ref. (Rakhmanov et al., 2001). This expression is a straightforward generalization of the corresponding formula for the conductivity obtained for the case of one-electron droplets (Rakhmanov et al., 2001). Electrical resistivity (1) exhibits a thermoactivation behavior where activation energy is equal to one half of the Coulomb repulsion energy (for details see Ref. (Rakhmanov et al., 2001)).

Expression (1) provides a fairly good description for the temperature dependence of the electrical resistivity for various manganites. As an illustration, in Figs. 1-4, we present experimental  $\rho(T)$  curves for six different materials. Experimental data are plotted for samples reported in Ref. (Babushkina et al., 2003; Fisher et al., 2003; Wagner et al., 2002; Zhao et al., 2001). The authors of these papers kindly provided us by the detailed numerical data on their measurements. As it could be seen from the figures and their captions, the examined samples differ in their chemical composition, type of crystal structure, magnitude of electrical resistivity (at fixed temperature, the latter varies for different

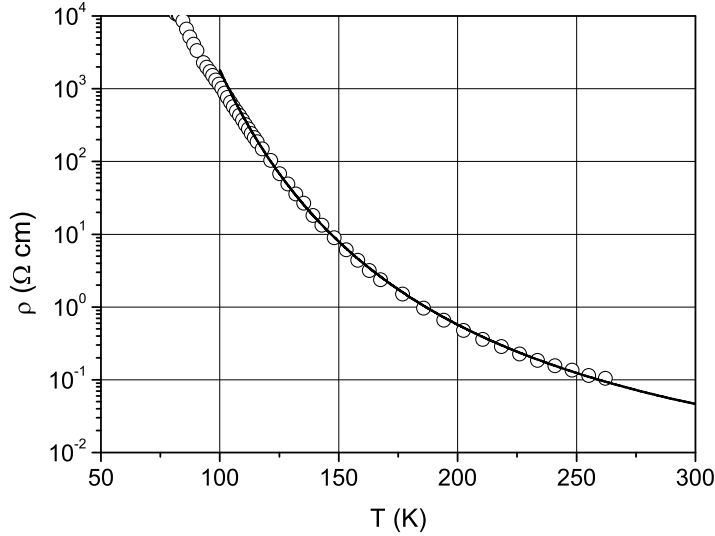


Figure 2. Temperature dependence of the resistivity for  $\text{Pr}_{0.71}\text{Ca}_{0.29}\text{MnO}_3$  sample (Fisher et al., 2003): experimental data (circles) and theoretical curve (solid line) based on Eq. (1).

samples by more than two orders of magnitude), and also by their low-temperature behavior (which is metallic for some samples and insulating for the others). On the other hand, in the high-temperature range (above the point of ferromagnetic phase transition),  $\rho(T)$  exhibits a similar behavior for all the samples, which is well fitted by the relationship  $\rho(T) \propto T \exp(A/2k_B T)$  (solid lines in the figures).

Based on Eq. (1) and experimental data, one can deduce some quantitative characteristics of the phase-separated state. In particular, the analysis carried out in the papers (Zhao et al., 2001; Zhao et al., 2002) demonstrated that an accurate estimate for the value of Coulomb energy  $A$  can be found by fitting experimental data and using Eq. (1). The data represented in Fig. 1-4 suggest that the Coulomb barrier  $A$  can be determined with an accuracy of 2-3% and its value lies in the narrow range from 3500 to 3700 K (see Table 1). As it was mentioned in the papers (Zhao et al., 2001; Rakhmanov et al., 2001; Zhao et al., 2002), the characteristic frequency  $\omega_0$  in (1) can also vary in a restricted range of  $10^{13}$ - $10^{14}$  Hz. This estimate might be derived, for example, from the uncertainty principle:  $\hbar\omega_0 \sim \hbar^2/2ma^2$ , where  $a$  is a characteristic droplet size, and  $m$  is the electron mass. Assuming  $a \sim 1 - 2$  nm, one

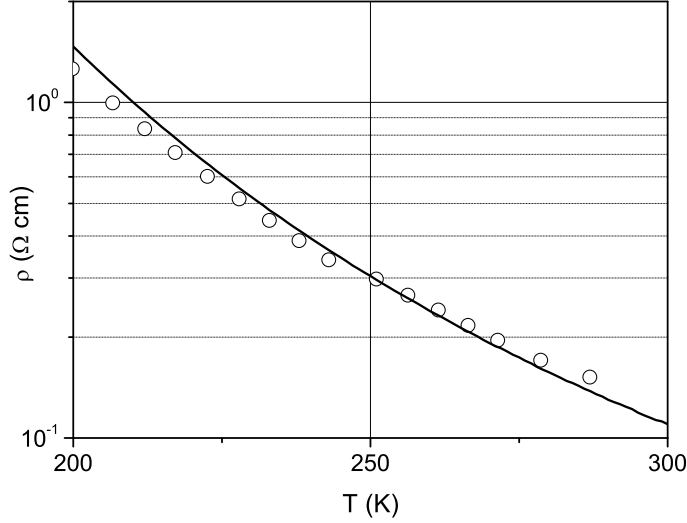


Figure 3. Temperature dependence of the resistivity for a layered manganite  $(\text{La}_{0.4}\text{Pr}_{0.6})_{1.2}\text{Sr}_{1.8}\text{Mn}_2\text{O}_7$  (Wagner et al., 2002): experimental data (circles) and theoretical curve (solid line) based on Eq. (1).

obtains the latter estimate. Note also that these values of a droplet size allow us to find an estimate for the barrier energy  $A$ , which is accurate within the order of magnitude. This energy is of the order of  $e^2/\varepsilon a$ , and substituting permittivity  $\varepsilon \sim 10$ , we get a value of  $A$  consistent with the experimental data.

Table 1.

Samples	$A$ , K	$\rho(200\text{ K})$ , $\Omega\text{-cm}$	$l^5 n^2 k$ , $\text{cm}^{-1}$	Data source
$(\text{La}_{1-y}\text{Pr}_y)_{0.7}\text{Ca}_{0.3}\text{MnO}_3$	3650	1.25	$2 \cdot 10^5$	Fig. 1 <sup>a)</sup>
$\text{Pr}_{0.71}\text{Ca}_{0.29}\text{MnO}_3$	3500	0.57	$3 \cdot 10^5$	Fig. 2 <sup>b)</sup>
$(\text{La}_{0.4}\text{Pr}_{0.6})_{1.2}\text{Sr}_{1.8}\text{Mn}_2\text{O}_7$ <sup>*)</sup>	3600	1.5	$1.5 \cdot 10^5$	Fig. 3 <sup>c)</sup>
$\text{La}_{0.8}\text{Mg}_{0.2}\text{MnO}_3$	3700	283	$1 \cdot 10^3$	Fig. 4 <sup>d)</sup>

<sup>a)</sup> (Babushkina et al., 2003)

<sup>b)</sup> (Fisher et al., 2003)

<sup>c)</sup> (Wagner et al., 2002)

<sup>d)</sup> (Zhao et al., 2001)

<sup>\*)</sup> The chemical formula of this composition can be written as  $(\text{La}_{0.4}\text{Pr}_{0.6})_{2-2x}\text{Sr}_{1+2x}\text{Mn}_2\text{O}_7$

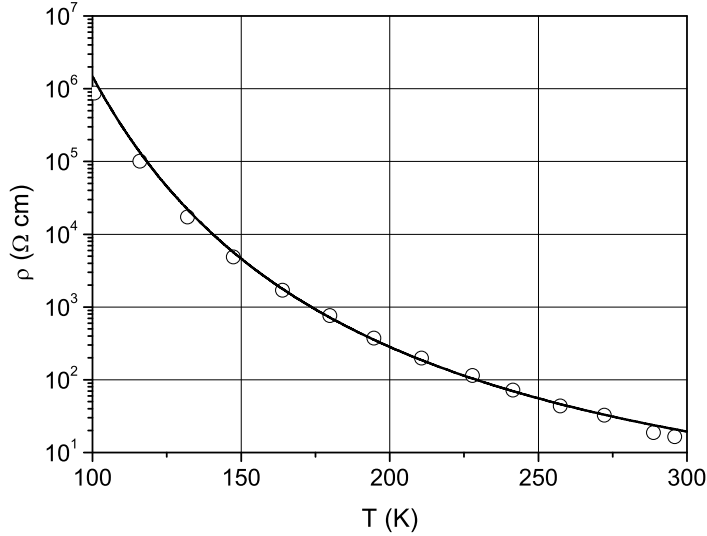


Figure 4. Temperature dependence of the resistivity for  $\text{La}_{0.8}\text{Mg}_{0.2}\text{MnO}_3$  sample (Zhao et al., 2001): experimental data (circles) and theoretical curve (solid line) based on Eq. (1).

It is rather difficult to estimate the tunnelling length  $l$ . However, we can say that in the domain of the applicability of relationship (1), length  $l$  cannot be much smaller than an interdroplet spacing (Rakhmanov et al., 2001). In another situation, the behavior of the resistivity would be different. In the quasiclassical approximation, the tunnelling length is of the order of the characteristic size for the wave function provided the barrier height is comparable with the depth of the potential well. In our case, the size of the electron wave function is of the order of a ferron size, while the height of the barrier practically coincides with the depth of the potential well. The latter naturally follows from the model of ferron formation (Nagaev, 2001). Therefore, it seems reasonable to assume the tunnelling length to be of the same order as a ferron size (few nanometers), though, generally speaking, it can substantially differ from  $a$ .

It is rather nontrivial task to estimate the concentration  $n$  of ferrons. In fact, following the papers (Zhao et al., 2001; Zhao et al., 2002), concentration  $n$  could be determined by the dopant concentration  $x$  as  $n \approx x/d^3$ . Yet this approach would bring at least two contradictions. First, even under the moderate concentration of divalent element

$x = 0.1 - 0.2$  the droplets should overlap giving rise to the continuous metallic and ferromagnetic cluster. However, the material could be insulating even at larger concentrations ( $x = 0.5 - 0.6$ ), at least, in a high-temperature range. Second, as it can be seen from the experimental data, the relation between a dopant concentration and the conductivity of manganites is relatively complicated - for some materials changing  $x$  by a factor of two can change resistivity by two orders of magnitude (Zhao et al., 2001; Zhao et al., 2002), for other materials  $\rho(x)$  exhibits even a nonmonotonic behavior in certain concentration ranges. Note that these discrepancies are essential not only for our model of phase separation but also for other models dealing with the properties of manganites (e.g., polaronic models (Ziese and Srinithiwarawong, 1998; Jakob et al., 1998)). Unfortunately, the authors of the papers (Zhao et al., 2001; Zhao et al., 2002) do not take into account these considerations when analyzing their results from the standpoint of the existing theories of the conductivity in manganites. The natural conclusion is that the number of carriers, which contribute to the charge transfer processes does not coincide with the concentration of the divalent dopant  $x$ . This is particularly obvious in the case of charge ordering when some part of the carriers introduced by doping becomes localized and forms a regular structure.

Therefore, using expression (1) and experimental data, we are able to obtain also the value of the combination  $l^5 n^2 k$ . In Table 1, the values of Coulomb energy  $A$ , resistivity  $\rho$  at 200 K and, combination  $l^5 n^2 k$  are presented. All estimations were made based on Eq. (1) and the experimental data of Fig. 1-4. Note that whereas the accuracy of the estimate for  $A$  is about  $\pm 50$  K, the combination  $l^5 n^2 k$  could be estimated only by the order of magnitude (at least, due to the uncertainty in the values of frequency  $\omega_0$ ).

### 3. Magnetoresistance

In the papers (Babushkina et al., 2003; Sboychakov et al., 2002; Sboychakov et al., 2003), it was demonstrated that the model of phase separation considered here results in a rather specific dependence of the magnetoresistance  $MR(T, H)$  on temperature and magnetic field. At relatively high temperatures and not very strong magnetic fields, the expression for the magnetoresistance reads

$$MR \approx 5 \cdot 10^{-3} \frac{\mu_B^3 S^5 N_{ef}^3 Z^2 g^3 J^2 H_a}{(k_B T)^5} H^2, \quad (2)$$



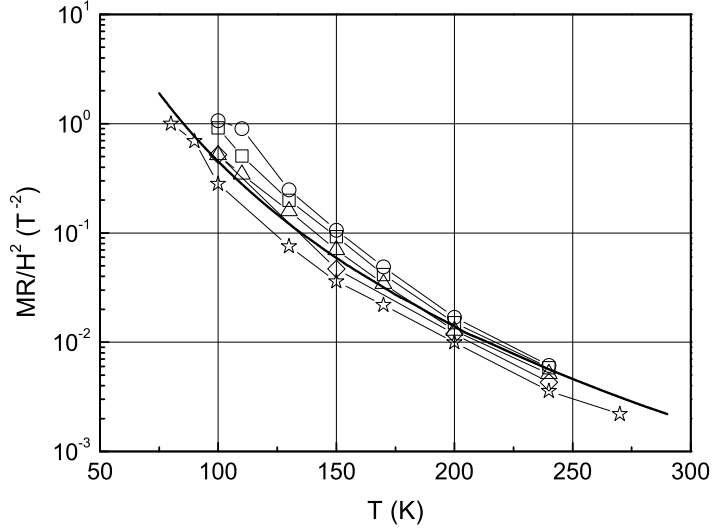


Figure 5. Temperature dependence of  $MR/H^2$  ratio for  $(La_{1-y}Pr_y)_{0.7}Ca_{0.3}MnO_3$  samples (Babushkina et al., 2003). Squares, triangles, circles, diamonds, and asterisks correspond to  $y = 0.75$ ,  $y = 0.75$  (with 30% of  $^{18}O$ ),  $y = 0.75$  (with  $^{16}O \rightarrow ^{18}O$  isotope substitution),  $y = 1$ , and  $y = 1$  (with  $^{16}O \rightarrow ^{18}O$  isotope substitution), respectively. Solid line is the fit based on Eq. (2) ( $MR \propto 1/T^5$ ).

where  $\mu_B$  is the Bohr magneton,  $S$  is the average spin of a manganese ion,  $N_{ef}$  is the number of manganese atoms in a droplet,  $Z$  is the number of nearest neighbors of a manganese ion,  $g$  is the Landé factor,  $J$  is the exchange integral of the ferromagnetic interaction, and  $H_a$  is the effective field of magnetic anisotropy of a droplet. The  $MR \propto H^2/T^5$  dependence was observed in the experiments for a number of manganites in the region of their non-metallic behavior (Babushkina et al., 2003; Fisher et al., 2003). The same high-temperature behavior of the magnetoresistance can be obtained by processing the experimental data reported in Ref. (Wagner et al., 2002; Zhao et al., 2001) (see Figs. 5-8).

The value of  $S$  depends on the relative content of a trivalent and a tetravalent manganese ions and ranges from  $3/2$  to  $2$ . Below it is assumed that  $S = 2$  for all the estimations. Parameter  $Z$  is, in fact, the number of manganese ions interacting with a conduction electron placed in a droplet. It is reasonable to assume that  $Z$  is of the order of the number of nearest-neighbor sites around a manganese ion, i.e.

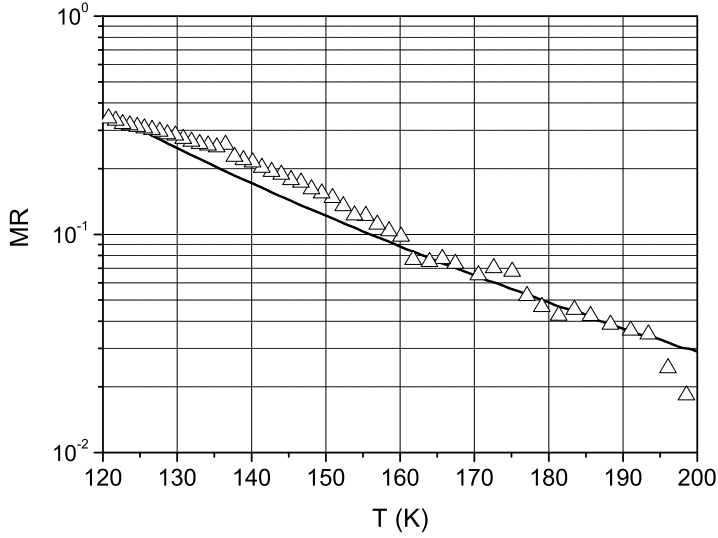


Figure 6. Temperature dependence of the magnetoresistance for  $\text{Pr}_{0.71}\text{Ca}_{0.29}\text{MnO}_3$  sample at  $H = 2\text{T}$ : experimental data (triangles) (Fisher et al., 2003) and theoretical curve (solid line) based on Eq. (2).

$Z \approx 6$ . The Landé factor  $g$  is determined from the experimental data. For manganese,  $g$  is usually assumed to be close to its spin value 2. The exchange integral  $J$  characterizes the magnetic interaction between a conduction electron and the molecular field generated by ferromagnetically correlated spins in a droplet. It is this molecular field that produces

Table 2.

Samples	$N_{ef}$	$x$	$k$	Data source
$(\text{La}_{1-y}\text{Pr}_y)_{0.7}\text{Ca}_{0.3}\text{MnO}_3$	250	0.3	75	Fig. 5 <sup>a)</sup>
$\text{Pr}_{0.71}\text{Ca}_{0.29}\text{MnO}_3$	200	0.29	58	Fig. 6 <sup>b)</sup>
$(\text{La}_{0.4}\text{Pr}_{0.6})_{1.2}\text{Sr}_{1.8}\text{Mn}_2\text{O}_7$ <sup>*</sup>	250	0.4	100	Fig. 7 <sup>c)</sup>
$\text{La}_{0.8}\text{Mg}_{0.2}\text{MnO}_3$	265	0.2	53	Fig. 8 <sup>d)</sup>

<sup>a)</sup> (Babushkina et al., 2003)

<sup>b)</sup> (Fisher et al., 2003)

<sup>c)</sup> (Wagner et al., 2002)

<sup>d)</sup> (Zhao et al., 2001)

<sup>\*</sup> The chemical formula of this composition can be written as  $(\text{La}_{0.4}\text{Pr}_{0.6})_{2-2x}\text{Sr}_{1+2x}\text{Mn}_2\text{O}_7$

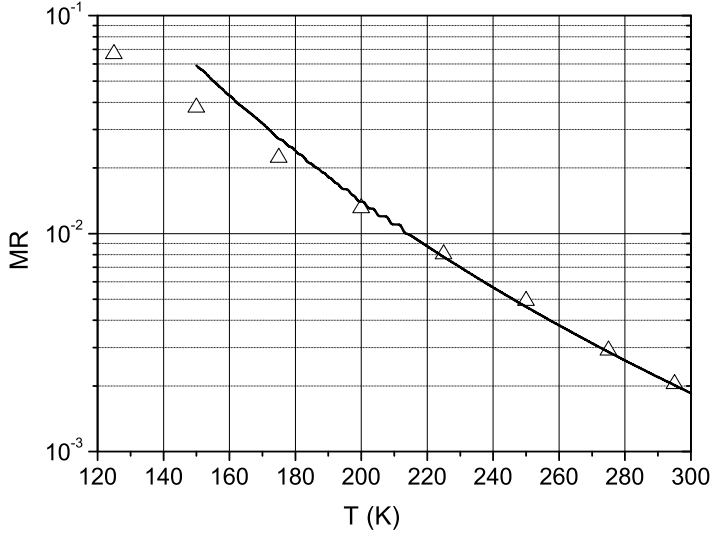


Figure 7. Temperature dependence of the magnetoresistance for  $(\text{La}_{0.4}\text{Pr}_{0.6})_{1.2}\text{Sr}_{1.8}\text{Mn}_2\text{O}_7$  sample at  $H = 1\text{T}$ : experimental data (triangles) (Wagner et al., 2002) and theoretical curve (solid line) based on Eq. (2).

a ferromagnetic state at low temperatures. Therefore, we can use a well-known relationship  $S(S+1)ZJ/3 = k_B T_C$  of the molecular field theory to evaluate the exchange integral (here  $T_C$  is the Curie temperature). The value of  $T_C$  is determined from the experiment (based on neutron diffraction or magnetization measurements). For example, in La-Pr-Ca manganites, it is about 100 – 120 K (Balagurov et al., 2001).

The magnetic anisotropy of manganites related to crystal structure of these compounds is usually not too high. This implies that the main contribution to the effective field of a magnetic anisotropy  $H_a$  stems from the shape anisotropy of a droplet and can be evaluated as  $H_a = \pi(1 - 3\tilde{N})M_s$ , where  $\tilde{N}$  is the demagnetization factor of the droplet (along the main axis),  $M_s$  is the magnetic moment per unit volume of the droplet. Below we assume a droplet to be sufficiently elongated ( $\tilde{N} \ll 1$ ) and  $M_s = Sg\mu_B/d^3$ . Then  $H_a \approx 2$  kOe.

The value of  $N_{ef}$  is determined by the size of a droplet and it could be found from the neutron diffraction experiments. However, we are unaware of such measurements performed for the systems under discussion in a wide temperature range. Therefore,  $N_{ef}$  is treated here as a fitting parameter. Hence, using Eq. (2) and the above estimates, we can deter-

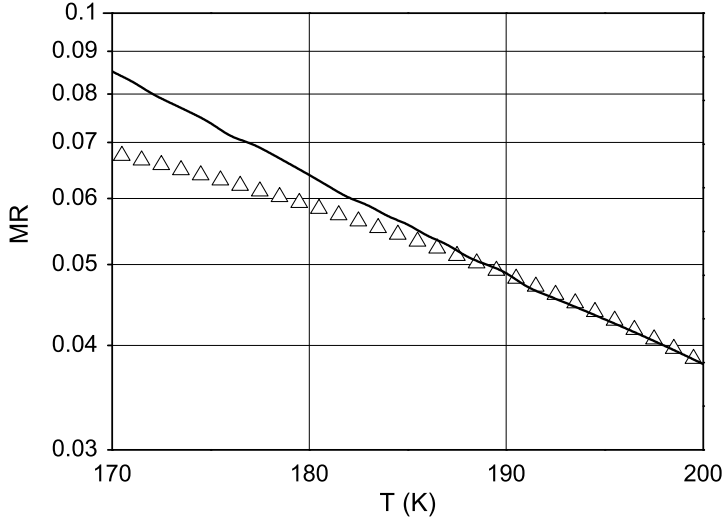


Figure 8. Temperature dependence of the magnetoresistance for  $\text{La}_{0.8}\text{Mg}_{0.2}\text{MnO}_3$  sample at  $H = 1.5\text{T}$ : experimental data (triangles) (Zhao et al., 2001) and theoretical curve (solid line) based on Eq. (2).

mine the value of  $N_{ef}$  from the experimental data on the magnetoresistance (in the range of parameters corresponding to  $MR \propto H^2/T^5$ ). The results are summarized in Table 2. In Figs. 5-8, solid curves correspond to the fitting procedure based on Eq. (2). The value of  $T_C$  was chosen to be equal to 120 K.

As a result, the size of the ferromagnetically correlated regions turns out to be nearly the same at temperatures about 200-300 K for all compositions under discussion. The volume of these regions is approximately equal to that of a ball with 7-8 lattice constants in diameter. It is natural to assume that within a droplet the number of charge carriers contributing to tunnelling processes equals to the number of dopant atoms. Hence, we can write that  $k = N_{ef}x$ , where  $x$  is the atomic percentage of dopants. The values of  $x$  and  $k$  are presented in Table 2.

#### 4. Magnetic susceptibility

The concentration of droplets can be evaluated based on the magnetic susceptibility data, if we assume that the dominant contribution to the susceptibility comes from the ferromagnetically correlated regions. At high temperatures ( $k_B T \gg \mu_B g S N_{ef} H, \mu_B g S N_{ef} H_a$ ), susceptibility

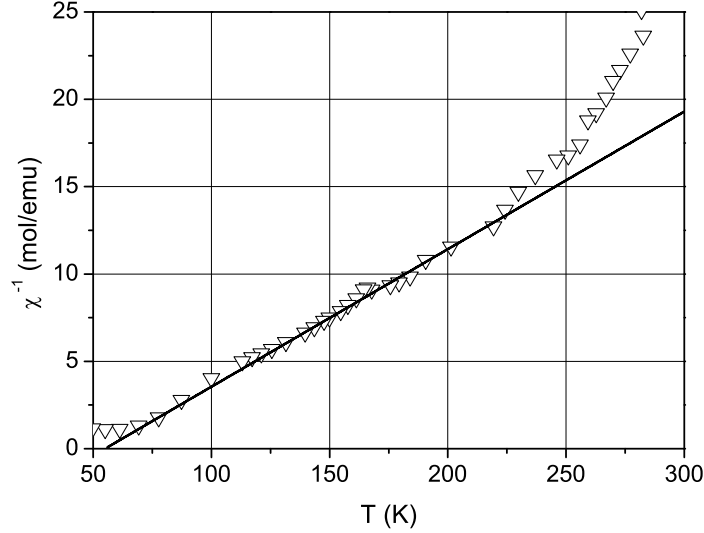


*Figure 9.* Temperature dependence of the inverse magnetic susceptibility for  $La_{1-y}Pr_y)_{0.7}Ca_{0.3}MnO_3$  sample at  $y = 1$ : experimental data (triangles) (Babushkina et al., 2003) and theoretical curve (solid line) based on Eq. (3). For the other samples of this group, the behavior of  $\chi(T)$  at high temperatures is rather similar to that illustrated in this figure (see Ref. (Babushkina et al., 2003)).

$\chi(T)$  can be written as

$$\chi(T) = \frac{n(\mu_B g S N_{ef})^2}{3k_B(T - \Theta)}, \quad (3)$$

*Table 3.*

<i>Samples</i>	$\Theta$ , K	$n$ , $cm^{-3}$	$p$	$l$ , $\text{\AA}$	<i>Data source</i>
$(La_{1-y}Pr_y)_{0.7}Ca_{0.3}MnO_3$	55	$1.8 \cdot 10^{18}$	0.03	24	Fig. 9 <sup>a)</sup>
$Pr_{0.71}Ca_{0.29}MnO_3$	105	$6.0 \cdot 10^{18}$	0.07	17	Fig. 10 <sup>b)</sup>
$(La_{0.4}Pr_{0.6})_{1.2}Sr_{1.8}Mn_2O_7$ <sup>*)</sup>	255	$2.5 \cdot 10^{18}$	0.04	19	Fig. 11 <sup>c)</sup>
$La_{0.8}Mg_{0.2}MnO_3$	150	$0.6 \cdot 10^{18}$	0.01	14	Fig. 12 <sup>d)</sup>

<sup>a)</sup> (Babushkina et al., 2003)

<sup>b)</sup> (Fisher et al., 2003)

<sup>c)</sup> (Wagner et al., 2002)

<sup>d)</sup> (Zhao et al., 2001)

<sup>\*)</sup> The chemical formula of this composition can be written as  $(La_{0.4}Pr_{0.6})_{2-2x}Sr_{1+2x}Mn_2O_7$

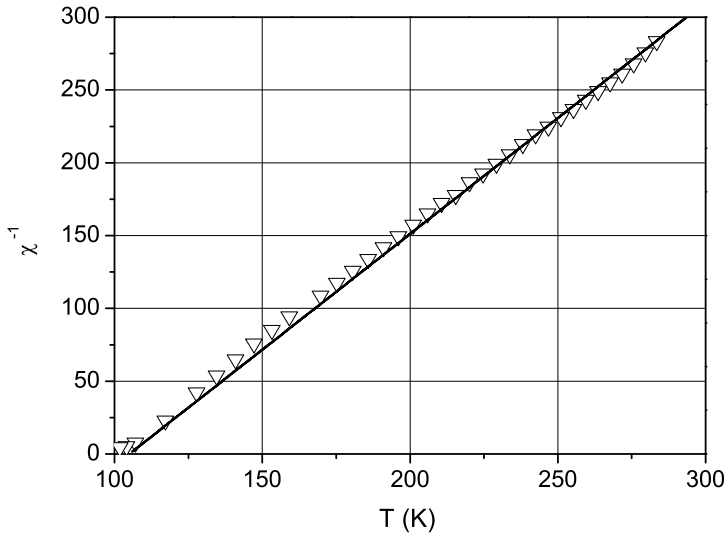


*Figure 10.* Temperature dependence of the inverse magnetic susceptibility for  $\text{Pr}_{0.71}\text{Ca}_{0.29}\text{MnO}_3$  sample: experimental data (triangles) (Fisher et al., 2003) and theoretical curve (solid line) based on Eq. (3). The sample was porous, its density was assumed to differ by a factor of 0.7 from the theoretical value.

where  $\Theta$  is the Curie-Weiss constant. The results of the processing of the experimental data are presented in Table 3. In Figs. 9-12, the solid curves correspond to the fitting procedure based on Eq. (3). Using these results, we can also estimate the concentration of ferromagnetic phase as  $p = nN_e f d^3$ . For all the samples, the value of the lattice constant  $d$  was taken to be equal to  $3.9 \text{ \AA}$ . Based on the data of Tables 1-3, it is also possible to find an estimate for the tunnelling length  $l$ .

## 5. Discussion

To sum up, the analysis performed in the previous sections demonstrates that a simple model of the electron tunnelling between the ferromagnetically correlated regions (FM droplets) provides a possibility to describe the conductivity and the magnetoresistance data for a wide class of manganites. The comparison of the theoretical predictions with the experimental data on the temperature dependence of the resistivity, magnetoresistance, and magnetic susceptibility enables us to reveal various characteristics of the phase-separated state such as the size of

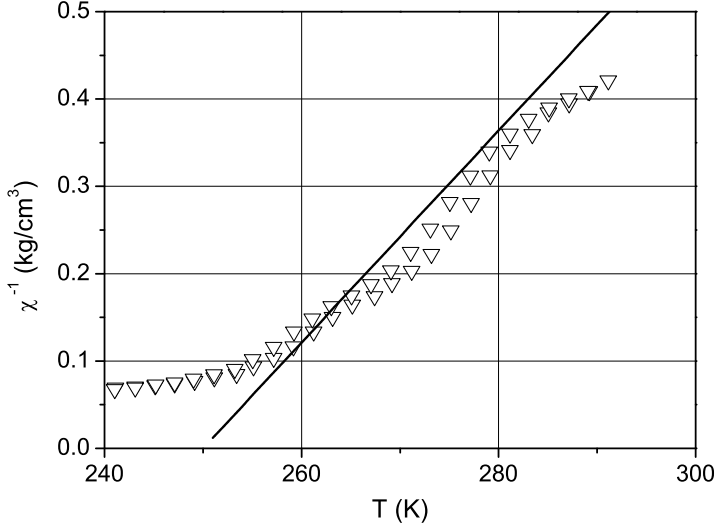


Figure 11. Temperature dependence of the inverse magnetic susceptibility for the sample of  $(\text{La}_{0.4}\text{Pr}_{0.6})_{1.2}\text{Sr}_{1.8}\text{Mn}_2\text{O}_7$ -layered manganite: experimental data (triangles) (Wagner et al., 2002) and theoretical curve (solid line) based on Eq. (3).

FM droplets, their density, the number of electrons in a droplet and also to estimate the characteristic tunnelling length of the charge carriers. The determined values of parameters appear to be rather reasonable. Indeed, the characteristic tunnelling length turns out to be of the order of FM droplet size, the concentration of the ferromagnetic phase in the high-temperature range is substantially smaller than the percolation threshold and varies from about 1% to 7%.

Note also that the droplets contain 50-100 charge carriers, whereas parameter  $A$  deduced from the experimental data is equal by the order of magnitude to the energy of Coulomb repulsion in a metallic ball of  $(7 \div 8)d$  in diameter. The obtained numerical values for the droplet parameters (characteristic tunnelling barrier, size, and tunnelling length) are close for manganites with drastically different transport properties.

The large magnitude of the  $1/f$  noise in the temperature range corresponding to the insulating state is another characteristic feature of the phase-separated manganites (Podzorov et al., 2000; Podzorov et al., 2001). In the framework of the model of phase separation discussed here, the following expression for the Hooge constant was derived in the

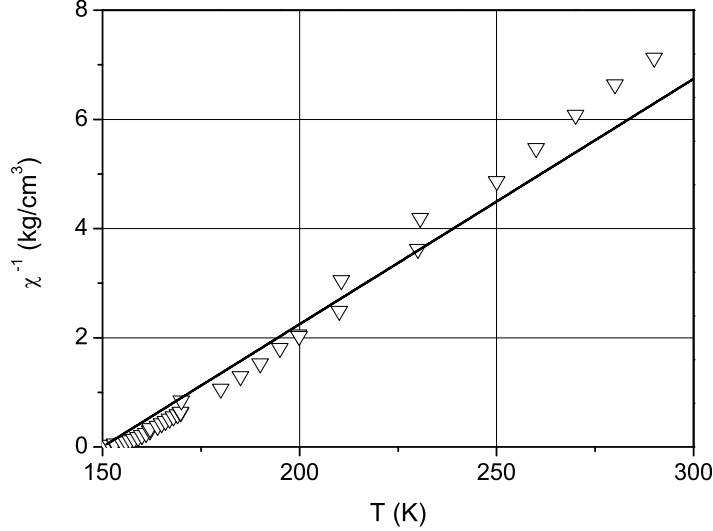


Figure 12. Temperature dependence of the inverse magnetic susceptibility for  $\text{La}_{0.8}\text{Mg}_{0.2}\text{MnO}_3$  sample: experimental data (triangles) (Zhao et al., 2001) and theoretical curve (solid line) based on Eq. (3).

papers (Rakhmanov et al., 2001; Sboychakov et al., 2002)

$$\alpha_H = \frac{\langle \delta U^2 \rangle_\omega V_s \omega}{U_{DC}^2} = 2\pi^2 l^3 \ln^2 \left( \frac{\tilde{\omega}_0}{\omega} \right), \quad (4)$$

where  $\langle \delta U^2 \rangle_\omega$  is the spectral density of the voltage fluctuations,  $V_s$  is the volume of a sample,  $U_{DC}$  is the applied voltage, and  $\tilde{\omega}_0 = \omega_0 \exp(A/2k_B T)$ . Substituting to Eq. (4) the estimated values of the parameters presented in the tables and in the text, we get  $\alpha_H \approx 10^{-16} \text{ cm}^3$  at temperatures 100-200 K and frequencies 1-1000  $\text{s}^{-1}$ . This value of  $\alpha_H$  is by 3-5 orders of magnitude higher than the corresponding values for semiconductors.

Thus, we have a rather consistent scheme describing the transport properties of manganites under condition that the ferromagnetically correlated regions do not form a percolation cluster. Moreover, the presented approach proves to be valid for a fairly wide range of the dopant concentrations. However, as it was mentioned above, the relation between the concentration of ferromagnetic droplets and the doping level is far from being well understood. If the picture of the phase separation is believed to be applicable, it becomes obvious that not all electrons or holes introduced by doping participate in the transport processes. Below we try to present some qualitative arguments illustrating the pos-



sible difference in the effective concentration of charge carriers below and above the transition from paramagnetic to magnetically ordered state.

In the phase diagram of a typical manganite, one would have the AFM state with FM-phase inclusions in the low-temperature range and at a low doping level. The transition from AFM to FM phase occurs upon doping. At high temperatures, manganites are in the paramagnetic (PM) state. When the temperature decreases, we observe the transition from PM to AFM or FM state depending on the doping level.

Let us consider the behavior of such a system in the vicinity of a triple point. In the AFM phase, radius  $R$  of a region which one electron converts into FM state can be estimated as  $R = d(\pi t/4J_{ff}S^2Z)^{1/5}$  (Kagan and Kugel, 2001), where  $J_{ff}$  is an AFM interaction constant. For high-temperature PM phase, a radius  $R_T$  of a region that one electron converts into FM state corresponds to the size of the so-called temperature ferron and equals to  $R_T = d(\pi t/4k_B T \ln(2S+1))^{1/5}$  (Kagan and Kugel, 2001). The critical concentration  $x_c \approx 0.15$  of the overlapping of low-temperature ferrons can be derived from the estimate  $x_c \approx 3/4\pi \cdot (d/R)^3$ , while for the high-temperature ferrons it follows from the estimate  $\delta_c \approx 3/4\pi \cdot (d/R_T)^3$ . Substituting the expressions for the radii of the high- and the low-temperature ferrons to the ratio  $x_c/\delta_c$ , we obtain the following estimate for this ratio in the vicinity of the triple point corresponding to the coexistence of FM, AFM, and PM phases:

$$\frac{x_c}{\delta_c} \sim \left[ \frac{T \ln(2S+1)}{zJ_{ff}S^2} \right]^{3/5} \sim \left[ \frac{T_C \ln(2S+1)}{T_N} \right]^{3/5}, \quad (5)$$

where  $T_C$  and  $T_N$  are the Curie and the Neel temperatures, respectively. For the manganites under discussion, we have  $T_C \sim T_N \sim 120\text{-}150$  K and  $\ln(2S+1) \sim 1.6$  for  $S = 2$ , hence  $\delta_c \leq x_c$ . The sign of this inequality is in agreement with experimental data which imply  $\delta \sim 1 - 7\%$ . Thus, we do not have a clear explanation of the charge disbalance in paramagnetic region in spite of the fact that the trend is correctly caught by our simple estimates. Probably, at  $x > x_c$  (in real experiments the concentration  $x$  can be as high as 50%), the residual charge is localized in the paramagnetic matrix outside the temperature ferrons. The detailed study of this problem will be presented elsewhere.

## Acknowledgments

The authors are grateful to V.A. Aksenov, N.A. Babushkina, S.W. Cheong, I. Gordon, L.M. Fisher, D.I. Khomskii, F.V. Kusmartsev, V.V. Moshchalkov, A.N. Taldenkov, I.F. Voloshin, G. Williams and X.Z. Zhou for useful discussions and provided experimental data. This work

was supported by the Russian Foundation for Basic Research (Grants Nos. 02-02-16708, 03-02-06320, and NSh-1694.2003.2), INTAS (Grant No. 01-2008), and CRDF (Grant No. RP2-2355-MO-02).

## References

- Babushkina, N. A., Chistotina, E. A., Kugel, K. I., Rakhmanov, A. L., Gorbenko, O. Yu., and Kaul, A. R. (2003). *J. Phys.: Condens. Matter*, 15:259.
- Balagurov, A. M., Pomjakushin, V. Yu., Sheptyakov, D. V., Aksenov, V. L., Fischer, P., Keller, L., Gorbenko, O. Yu., Kaul, A. R., and Babushkina, N. A. (2001). *Phys. Rev. B*, 64:024420.
- Bulaevskii, L. N., Nagaev, E. L., and Khomskii, D. I. (1968). *Zh. Eksp. Teor. Fiz.*, 54:1562. [*Sov. Phys. JETP*, 27:836].
- Dagotto, E., Hotta, T., and Moreo, A. (2001). *Phys. Rep.*, 344:1.
- Fisher, L. M., Kalinov, A. V., Voloshin, I. F., Babushkina, N. A., Khomskii, D. I., and Kugel, K. I. (2003). *Phys. Rev. B*, 68:174403.
- Jakob, G., Westerburg, W., Martin, F., and Adrian, H. (1998). *Phys. Rev. B*, 58:14966.
- Kagan, M. Yu. and Kugel, K. I. (2001). *Usp. Fiz. Nauk*, 171:577. [*Physics Uspekhi*, 44:553].
- Lorenzana, J., Castellani, C., and Di Castro, C. (2001). *Phys. Rev. B*, 64:235128.
- Nagaev, E. L. (1967). *Pis'ma Zh. Eksp. Teor. Fiz.*, 6:484. [*JETP Lett.*, 6:18].
- Nagaev, E. L. (2001). *Phys. Rep.*, 346:387.
- Podzorov, V., Uehara, M., Gershenson, M. E., and Cheong, S-W. (2001). *Phys. Rev. B*, 64:115113.
- Podzorov, V., Uehara, M., Gershenson, M. E., Koo, T. Y., and Cheong, S-W. (2000). *Phys. Rev. B*, 61:R3784.
- Rakhmanov, A. L., Kugel, K. I., Blanter, Ya. M., and Kagan, M. Yu. (2001). *Phys. Rev. B*, 63:174424.
- Sboychakov, A. O., Rakhmanov, A. L., Kugel, K. I., Kagan, M. Yu., and Brodsky, I. V. (2002). *Zh. Eksp. Teor. Fiz.*, 122:869. [*JETP*, 95:753].
- Sboychakov, A. O., Rakhmanov, A. L., Kugel, K. I., Kagan, M. Yu., and Brodsky, I. V. (2003). *J. Phys.: Condens. Matter*, 15:1705.
- Solin, N. I., Mashkautsan, V. V., Korolev, A. V., Loshkareva, N. N., and Pinsard, L. (2003). *Pis'ma Zh. Eksp. Teor. Fiz.*, 77:275. [*JETP Lett.*, 77:230].
- Wagner, P., Gordon, I., Moshchalkov, V. V., Bruynseraede, Y., Apostu, M., Suryanarayanan, R., and Revcolevschi, A. (2002). *Europhys. Lett.*, 58:285.
- Zhao, J. H., Kunkel, H. P., Zhou, X. Z., and Williams, G. (2001). *J. Phys.: Condens. Matter*, 13:285.
- Zhao, J. H., Kunkel, H. P., Zhou, X. Z., and Williams, G. (2002). *Phys. Rev. B*, 66:184428.
- Ziese, M. and Srinithiwarawong, C. (1998). *Phys. Rev. B*, 58:11519.